

**Supplementary Information to “Localized performance of riblets with curved cross-sectional profiles in boundary layers past finite length bodies”**

**Shuangjiu Fu and Shabnam Raayai-Ardakani**

SI.1. Distribution of the  $\lambda^+$  and  $A^+$  for the riblets

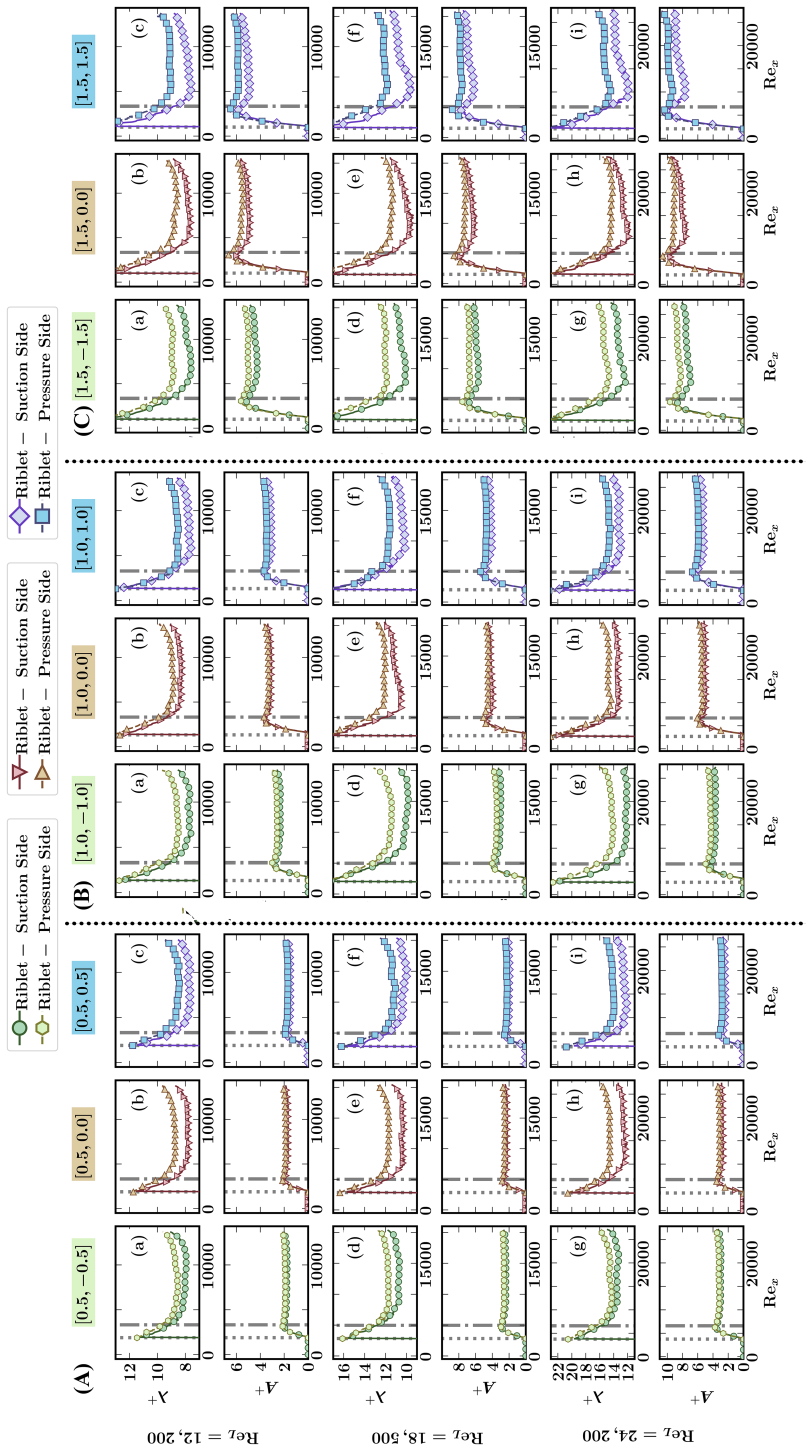


Figure SI.1: Distribution of  $\lambda^+$  and  $A^+$  for all the riblet samples of (A)  $\mathcal{R} = 0.5$ , (B)  $\mathcal{R} = 1.0$ , and (C)  $\mathcal{R} = 1.5$  for all the Reynolds numbers, calculated using the spanwise-averaged shear stress measured. Each row corresponds to a specific Reynolds number and each column corresponds to specific samples as marked. A similar tabular format is used in the upcoming figures as well. Locations of  $x_{LET}$  and  $x_{Flat}$  are marked by grey dotted and dash-dotted vertical lines.

## SI.2. Local control volume analysis inside the grooves for obtaining spanwise-averaged wall shear stress

Since we do not have access to the velocity profiles inside the grooves to capture the shear stress distribution, we use a simple control volume, bounded by the riblet wall on the bottom, and cut at the peak level of  $n = 0$ , with an infinitesimal depth of  $\delta x$ , such as the one shown in figure SI.2(b). Using this, we can write

$$-\int_x^{x+\delta x} \int_0^\lambda \tau_{n=0}(x, n=0, z) dz dx + \int_x^{x+\delta x} \int_{\text{riblet}} \tau_w d\ell dx + \int_{\text{inlet/Outlet}} p(x) - p(x + \delta x) dS = \sum_i \int_{S_i} \rho \mathbf{u}(\mathbf{u} \cdot \mathbf{n}_S) dS_i \quad (\text{SI.2.1})$$

where  $\tau_{n=0}$  is the shear stress distribution on the top boundary which is included instead of the cut,  $\tau_w$  is the shear stress distribution on the riblet wall,  $p$  is the pressure, and  $\mathbf{n}_S$  is the unit normal to the wall of the boundaries of control surfaces, and  $i \in [\text{Top, Inlet, Outlet, Riblet}]$ . For this control volume, at the limit of  $\delta x \rightarrow 0$  on the top boundary at  $n = 0$

$$\int_x^{x+\delta x} \int_0^\lambda (\rho uv) dz dx \approx 0 \quad (\text{SI.2.2})$$

and we also assume that with the slow down of the flow inside the grooves, between the inlet and outlet the variations in the velocity and pressure inside the grooves are also very small  $u(x; y, z) \approx u(x + \delta x; y, z)$  and  $p(x; y, z) \approx p(x + \delta x; y, z)$  and

$$\int_{\text{inlet}, x} (\rho u^2) dS \approx \int_{\text{outlet}, x+\delta x} (\rho u^2) dS \quad (\text{SI.2.3})$$

$$\int_{\text{inlet/Outlet}} p(x) - p(x + \delta x) dS \approx 0 \quad (\text{SI.2.4})$$

Thus,

$$-\int_x^{x+\delta x} \int_0^\lambda \tau_{n=0}(x, z) dz dx + \int_x^{x+\delta x} \int_{\text{riblet}} \tau_w d\ell dx = 0 \quad (\text{SI.2.5})$$

and

$$\langle \tau_{n=0} \rangle(x) = \frac{\int_0^\lambda \tau_{n=0}(x, z) dz}{\lambda} \approx \frac{\int_{\text{riblet}} \tau_w(\ell) d\ell}{\lambda} = \langle \tau_w \rangle. \quad (\text{SI.2.6})$$

Hence, just by having access to the average shear stress on the plane at the  $n = 0$ , we can evaluate the spanwise-averaged shear stress experienced by the riblet surface.

To test for the impact of the eliminated terms in the control volume analysis inside the grooves, we use the magnitudes of the PIV data right outside the grooves as upper-bounds of the distribution of the magnitude of the variables inside the grooves (with the other bound being zero) in the following format:

For the momentum term crossing the inlet/outlets, using the RHS of equation (SI.2.1), at the limit of  $\delta x \rightarrow 0$  we use the Taylor expansion:

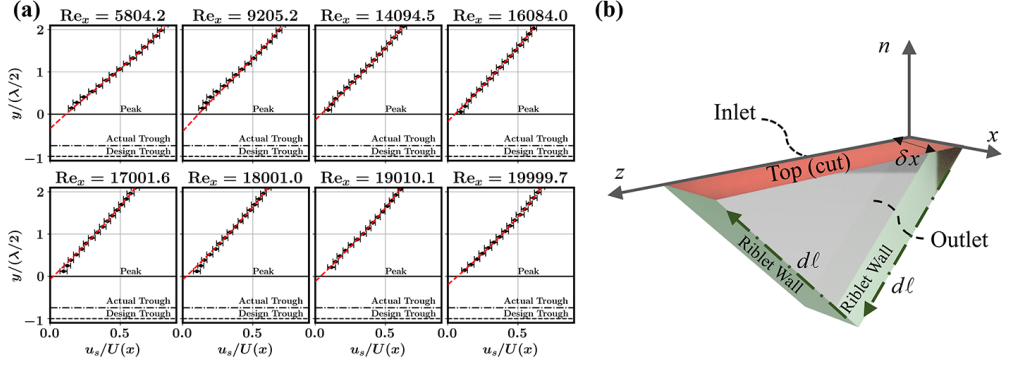


Figure SI.2: (a) Distribution of the tangential velocity profiles and their 95% confidence intervals, at 8 different location along the suction side of the [1.0, 0.0] sample at  $Re_L = 18,500$ , and the FS fits to the profiles and the extrapolations below the peak levels showing the location of  $n_0$ . Dashed and dash-dotted black lines correspond to the design and measured location of the troughs respectively. (b) A control volume inside the riblets, cut at the peak of the grooves with a thickness of  $\delta x$  in the  $x$  direction.

$$\rho \int_S (u(x + \delta x)^2 - u(x)^2) dS = \rho \int_S \left( u(x) \frac{\partial u(x)}{\partial x} \delta x + \mathcal{O}(\delta x^2) \right) dS \approx \rho \delta x \int_S u(x) \frac{\partial u(x)}{\partial x} dS \quad (\text{SI.2.7})$$

Since we don't have access to the  $u(x, y, z)$  inside the grooves, we use magnitude of

$$\langle u_{n=0} \rangle \frac{\partial \langle u_{n=0} \rangle}{\partial x} = \langle u \rangle (x, n=0) \frac{\partial \langle u \rangle}{\partial x} \Big|_{(x, n=0)} \quad (\text{SI.2.8})$$

as the magnitude of the bound of this term and where considering the sign we get

$$\langle u_{n=0} \rangle \frac{\partial \langle u_{n=0} \rangle}{\partial x} \geq 0 \Rightarrow 0 \leq \left( u(x) \frac{\partial u(x)}{\partial x} \right) \leq \left( \langle u_{n=0} \rangle \frac{\partial \langle u_{n=0} \rangle}{\partial x} \right) \quad (\text{SI.2.9})$$

$$\langle u_{n=0} \rangle \frac{\partial \langle u_{n=0} \rangle}{\partial x} \leq 0 \Rightarrow \left( \langle u_{n=0} \rangle \frac{\partial \langle u_{n=0} \rangle}{\partial x} \right) \leq \left( u(x) \frac{\partial u(x)}{\partial x} \right) \leq 0. \quad (\text{SI.2.10})$$

We find this velocity using the PIV results and assuming the entire distribution within the area "S" is captured by either of the bounds, the integral of equation (SI.2.7) is bounded by

$$\langle u_{n=0} \rangle \frac{\partial \langle u_{n=0} \rangle}{\partial x} \geq 0 \Rightarrow 0 \leq \rho \delta x \int_S \left( u(x) \frac{\partial u(x)}{\partial x} \right) dS \leq \rho \left( \langle u_{n=0} \rangle \frac{\partial \langle u_{n=0} \rangle}{\partial x} \right) \delta x S \quad (\text{SI.2.11})$$

$$\langle u_{n=0} \rangle \frac{\partial \langle u_{n=0} \rangle}{\partial x} \leq 0 \Rightarrow \rho \left( \langle u_{n=0} \rangle \frac{\partial \langle u_{n=0} \rangle}{\partial x} \right) \delta x S \leq \rho \delta x \int_S \left( u(x) \frac{\partial u(x)}{\partial x} \right) dS \leq 0 \quad (\text{SI.2.12})$$

where  $S$  is the cross-sectional area of the riblets.

For the pressure gradient, similarly, using third term of the LHS of equation (SI.2.1), at the limit of  $\delta x \rightarrow 0$ , we use the Taylor expansion:

$$\int_S p(x) - p(x + \delta x) dS = \int_S \left( \frac{\partial p}{\partial x} \delta x + \mathcal{O}(\delta x^2) \right) dS \approx \delta x \int_S \left( \frac{\partial p}{\partial x} \right) dS \quad (\text{SI.2.13})$$

Here, while we don't have access to measurements inside the groove, we use the pressure information from the same horizontal line (parallel to the Flat portion of the samples) discussed in section 3.4.1 of the manuscript as calculated using the procedure described in section 2.4.3. The line is at a height of  $y = \pm 0.6h$  which is at a distance of  $0.1h$  or  $\lambda/2$  from the Flat part of the surface on either side, where the 3D effects of the riblets have mostly faded away and it is safe to assume that  $\mathbf{u}(x, y, z) = \langle \mathbf{u} \rangle(x, y)$  and  $p(x, y, z) = \langle p \rangle(x, y)$ . We use this as the magnitude of the bound of the pressure distribution inside the grooves. Thus, with the substantial slow down of the flow inside the grooves as discussed, we assume the pressure is bounded between the

$$\left. \frac{\partial p}{\partial x} \right|_{y=\pm 0.6h} \geq 0 \Rightarrow 0 \leq \frac{\partial p(x, y, z)}{\partial x} \leq \left. \frac{\partial p}{\partial x} \right|_{y=\pm 0.6h} \quad (\text{SI.2.14})$$

$$\left. \frac{\partial p}{\partial x} \right|_{y=\pm 0.6h} \leq 0 \Rightarrow \left. \frac{\partial p}{\partial x} \right|_{y=\pm 0.6h} \leq \frac{\partial p(x, y, z)}{\partial x} \leq 0 \quad (\text{SI.2.15})$$

and thus equation (SI.2.13) is written as

$$\left. \frac{\partial p}{\partial x} \right|_{y=\pm 0.6h} \geq 0 \Rightarrow 0 \leq \delta x \int_S \left( \frac{\partial p}{\partial x} \right) dS \leq \delta x S \left. \frac{\partial p}{\partial x} \right|_{y=\pm 0.6h} \quad (\text{SI.2.16})$$

$$\left. \frac{\partial p}{\partial x} \right|_{y=\pm 0.6h} \leq 0 \Rightarrow \delta x S \left. \frac{\partial p}{\partial x} \right|_{y=\pm 0.6h} \leq \delta x \int_S \left( \frac{\partial p}{\partial x} \right) dS \leq 0. \quad (\text{SI.2.17})$$

For the contribution of the velocity in the normal direction, on the top boundary of the control volume, we can use a trapezoidal integration

$$\begin{aligned} \rho \int_0^\lambda \int_x^{x+\delta x} uv dx dz &\approx \rho \int_0^\lambda \frac{u(x + \delta x)v(x + \delta x) + u(x)v(x)}{2} \delta x dz \\ &\approx \rho \int_0^\lambda (u(x)v(x)\delta x + \mathcal{O}(\delta x^2)) dz \approx \rho \int_0^\lambda u(x)v(x) dz \delta x \end{aligned} \quad (\text{SI.2.18})$$

where using the Cauchy-Schwarz inequality we can write

$$\rho \left| \int_0^\lambda u(x)v(x) dz \right| \delta x \leq \rho \left| \int_0^\lambda u(x) dz \right| \left| \int_0^\lambda v(x) dz \right| \delta x \quad (\text{SI.2.19})$$

$$\rho \delta x \left| \langle uv \rangle(x, n=0) \right| \leq \rho \delta x \left| \langle v \rangle(x, n=0) \right| \left| \langle u \rangle(x, n=0) \right| = \rho \delta x \langle u_{n=0} \rangle \left| \langle v_{n=0} \rangle \right| \quad (\text{SI.2.20})$$

Using these bounds and knowing from the results that  $\langle u \rangle(x, n=0) = \langle u_{n=0} \rangle \geq 0$ , equation (SI.2.18) is bounded by

$$\langle v_{n=0} \rangle \geq 0 \Rightarrow 0 \leq \rho \delta x \langle uv \rangle(x, n=0) \leq \rho \delta x \langle u_{n=0} \rangle \langle v_{n=0} \rangle \quad (\text{SI.2.21})$$

$$\langle v_{n=0} \rangle \leq 0 \Rightarrow \rho \delta x \langle u_{n=0} \rangle \langle v_{n=0} \rangle \leq \rho \delta x \langle uv \rangle(x, n=0) \leq 0 \quad (\text{SI.2.22})$$

As for the shear stress terms in equation (SI.2.1) in the appendix, first using the definition of the spanwise averaging we have

$$\int_0^\lambda \tau_{n=0} dz = \langle \tau_{n=0} \rangle \lambda \quad (\text{SI.2.23})$$

and now, substituting the two above terms into the first term of equation (SI.2.1) and using trapezoidal method for integration and Taylor expansion

$$\begin{aligned} \int_x^{x+\delta x} \int_0^\lambda (\tau_{n=0}) dz dx &= \int_x^{x+\delta x} \langle \tau_{n=0} \rangle \lambda dx \approx \frac{(\langle \tau_{n=0} \rangle(x) + \langle \tau_{n=0} \rangle(x + \delta x)) \delta x}{2} \lambda \\ &\approx \frac{2\langle \tau_{n=0} \rangle(x) \delta x + \frac{\partial \langle \tau_{n=0} \rangle(x)}{\partial x} \delta x^2}{2} \lambda \approx \langle \tau_{n=0} \rangle(x) \delta x \lambda + \mathcal{O}(\delta x^2) \end{aligned} \quad (\text{SI.2.24})$$

For the other shear stress term, with

$$\int_{\text{riblet}} \tau_w(\ell) d\ell = \langle \tau_w \rangle \lambda \quad (\text{SI.2.25})$$

for the second term on the LHS of equation (SI.2.1) we have

$$\int_x^{x+\delta x} \int_{\text{riblet}} \tau_w(\ell) d\ell dx = \int_x^{x+\delta x} \langle \tau_w \rangle \lambda dx \approx \langle \tau_w \rangle(x) \delta x \lambda + \mathcal{O}(\delta x^2) \quad (\text{SI.2.26})$$

Then, substituting all the above terms back into equation (SI.2.1) neglecting the  $\mathcal{O}(\delta x^2)$  and reorganizing we have

$$\langle \tau_w \rangle(x) - \langle \tau_{n=0} \rangle(x) = \frac{\rho}{\lambda} \int_S \left( u \frac{\partial u}{\partial x} + \frac{\partial p}{\partial x} \right) dS + \rho \langle uv \rangle = \mathcal{B} \quad (\text{SI.2.27})$$

Now, using the bounds found in equations (SI.2.12), (SI.2.11), (SI.2.16), (SI.2.16), (SI.2.21), and (SI.2.22), and the sign of each of the terms we can evaluate the bounds of  $\langle \tau_w \rangle(x) - \langle \tau_{n=0} \rangle(x)$  via the bounds of the  $\mathcal{B}$  and thus

$$\mathcal{B}_{\text{lower}}(x) + \langle \tau_{n=0} \rangle(x) \leq \langle \tau_w \rangle(x) \leq \mathcal{B}_{\text{upper}}(x) + \langle \tau_{n=0} \rangle(x). \quad (\text{SI.2.28})$$

Lastly, integrating the results on either side of the sample:

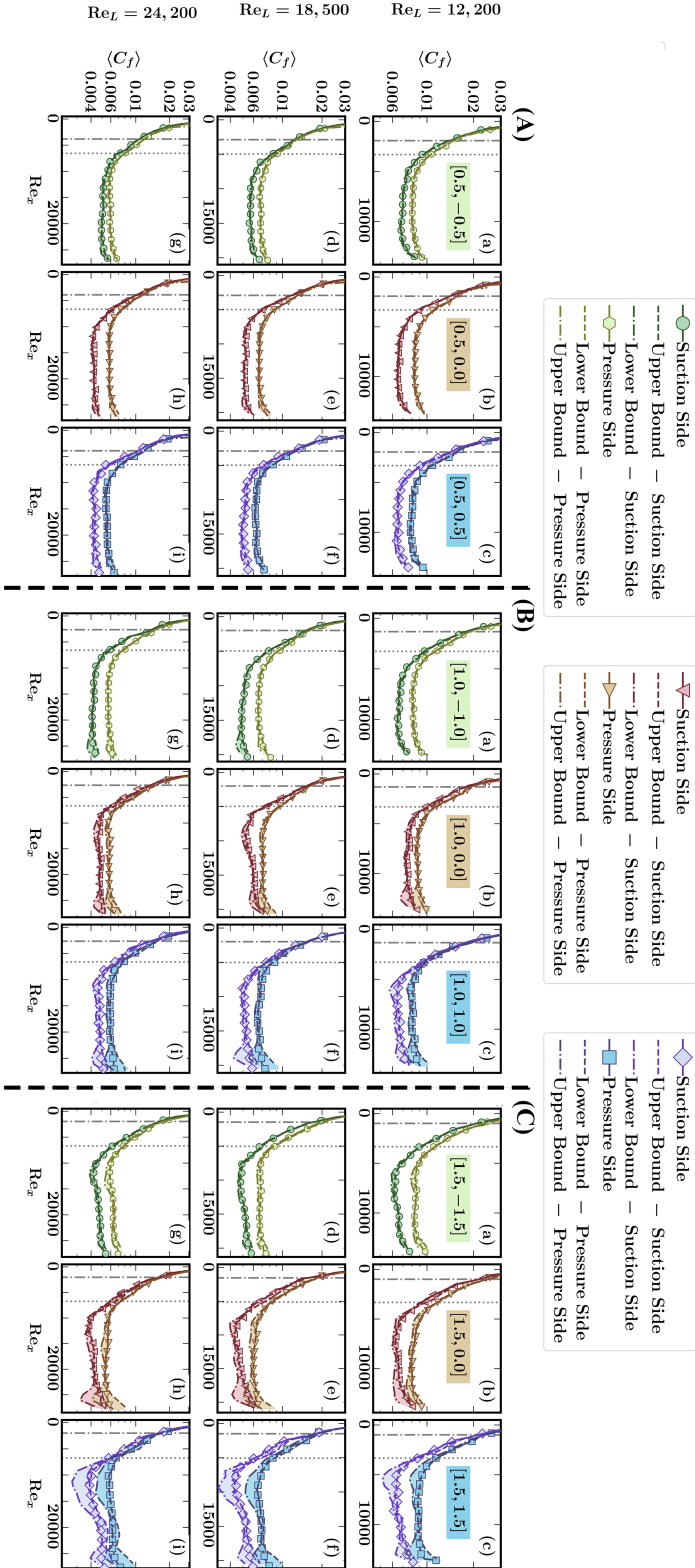
$$\int_0^L \left( \langle \tau_{n=0} \rangle^{\text{Front}} + \mathcal{B}_{\text{lower}}^{\text{Front}}(x) \right) dx \leq \int_0^L \langle \tau_w \rangle^{\text{Front}} dx \leq \int_0^L \left( \langle \tau_{n=0} \rangle^{\text{Front}} + \mathcal{B}_{\text{upper}}^{\text{Front}}(x) \right) dx \quad (\text{SI.2.29})$$

and

$$\int_0^L \left( \langle \tau_{n=0} \rangle^{\text{Back}} + \mathcal{B}_{\text{lower}}^{\text{Back}}(x) \right) dx \leq \int_0^L \langle \tau_w \rangle^{\text{Back}} dx \leq \int_0^L \left( \langle \tau_{n=0} \rangle^{\text{Back}} + \mathcal{B}_{\text{upper}}^{\text{Back}}(x) \right) dx \quad (\text{SI.2.30})$$

Using the above equations we plot  $\langle \tau_{n=0} \rangle$  and the upper and lower bounds in figure **SI.3**. We also add the sums of the integrals of the  $\mathcal{B}_{\text{upper}}^{\text{Front}}(x) + \mathcal{B}_{\text{upper}}^{\text{Back}}(x)$  and  $\mathcal{B}_{\text{lower}}^{\text{Front}}(x) + \mathcal{B}_{\text{lower}}^{\text{Back}}(x)$  as error-bars on the bar plots of the decomposed drag force as shown in figure 4 of the main text. As it can be seen from figures **SI.3** and 4 of the main text, even with consideration of upper/lower bounds for the momentum and pressure changes across a thin slice of the groove, the location of the bounds are very close to each other for shallow  $\mathcal{R} = 0.5$  riblet family. For the  $\mathcal{R} = 1.0$  family, a slight difference is visible, but mostly confined to the trailing edge of the body and more pronounced for the [1.0, 1.0] sample. For the sharpest  $\mathcal{R} = 1.5$  family, the [1.5, 0.0] and [1.5, 1.5] see larger differences between the upper and lower bounds, but they also have the largest cross-sectional riblet areas among all the samples. Again, to emphasize, *if the distributions of momentum and pressure could be replaced with the bounds for the entire  $S$* , then these are the bounds of the  $\langle \tau_w \rangle$ . However, we know that pressure and momentum components will have distributions as functions of  $(y, z)$  at every cross-section and the magnitude of the total integral of the terms over the cross-sectional area will be smaller than these bounds.

In addition, as it can be seen from figure 4 of the main text, the ultimate contributions of the upper and lower bounds to the integrals will have a limited effect on the  $C_D^f$  of the samples, and the largest effect is seen for the [1.5, 1.5] sample with the largest cross-sectional area. Note that the range of variation given by the error-bars of  $C_D^f$  are in the similar range or even smaller than 95% confidence intervals found for the profile drag and total drag. Thus, here, with the given PIV data available, we use  $\langle \tau_{n=0} \rangle$  to characterize the  $\langle C_f \rangle$  inside the grooves. Future experimental setups with 3D access to inside the grooves, or numerical simulations can further validate the above assumption.



SI.3. Distribution of the spanwise average shear stress and the percentage changes in the shear stress compared to the smooth reference

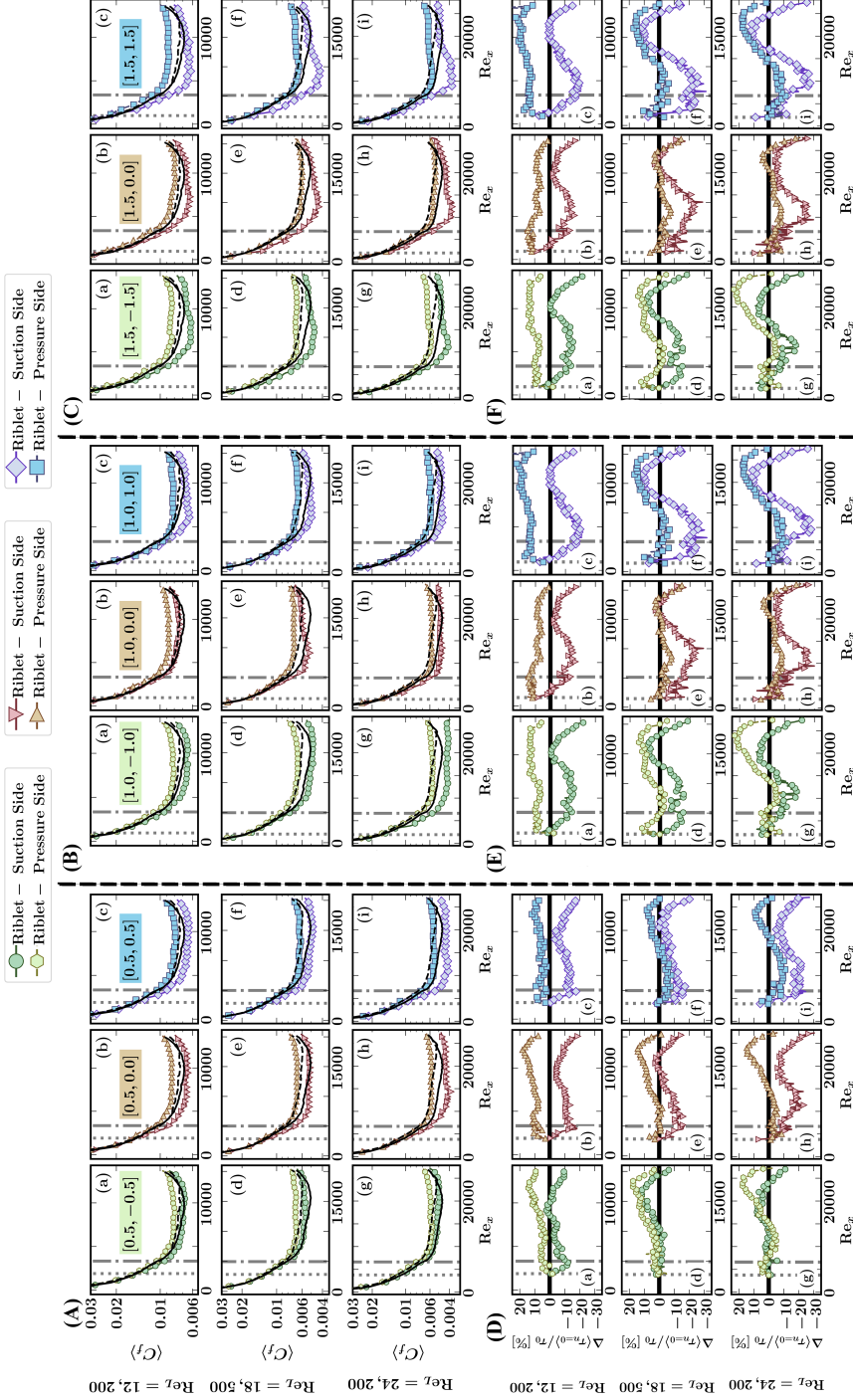


Figure SI.4: Distribution of  $\langle C_f \rangle(x)$  and the percentage of  $\Delta \langle \tau_{r=0} \rangle / \tau_0$  for all the riblet samples of (A) and (D)  $\mathcal{R} = 0.5$ , (B) and (E)  $\mathcal{R} = 1.0$ , and (C) and (F)  $\mathcal{R} = 1.5$  for all the Reynolds numbers. The  $C_{f,0}(x)$  of the reference smooth sample on the suction and pressure sides are shown with solid and dashed black lines respectively. Locations of  $x_{LET}$  and  $x_{Flat}$  are marked by grey dotted and dash-dotted vertical lines.

SI.4. Distribution of  $m$  parameter for all the samples

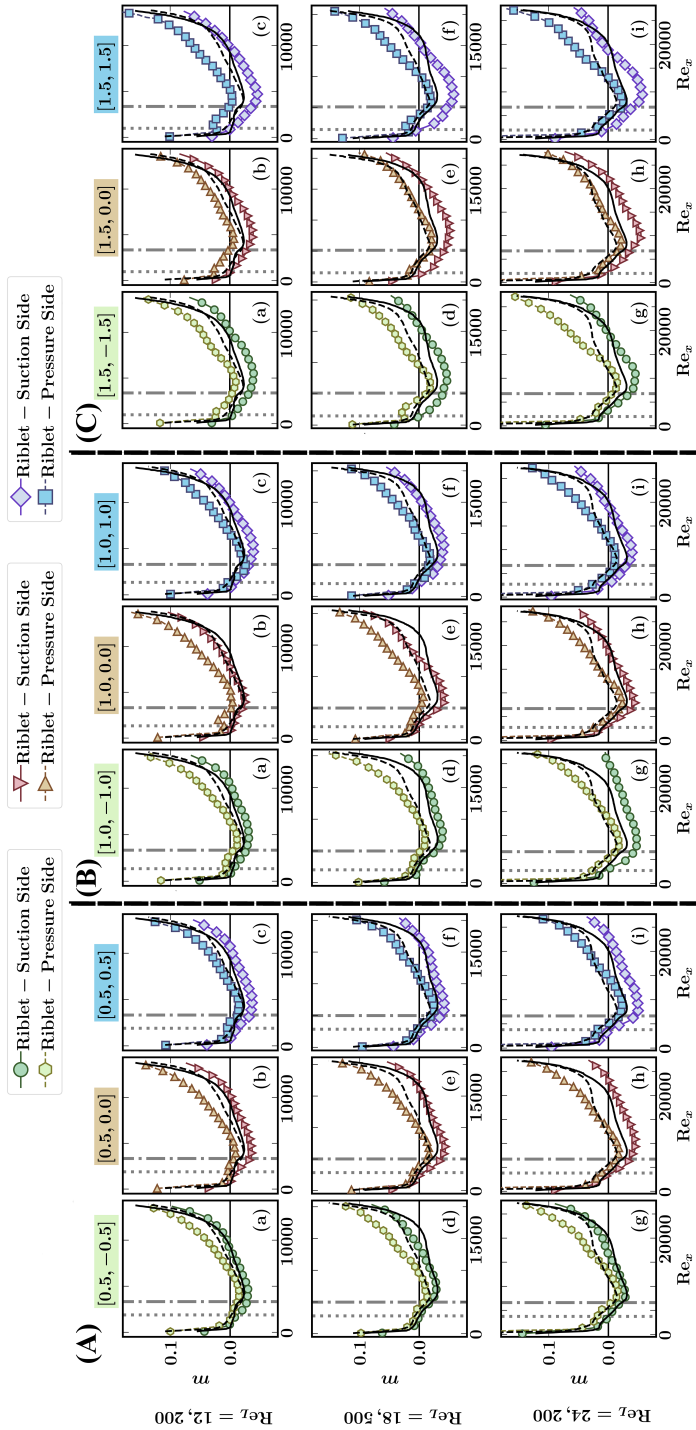


Figure SI.5: Distribution of  $m$  for all the riblet samples of (A)  $\mathcal{R} = 0.5$ , (B)  $\mathcal{R} = 1.0$ , and (C)  $\mathcal{R} = 1.5$  and the reference smooth samples, on the suction and pressure sides for all the tested Reynolds numbers. The  $m$  of the reference smooth sample on the suction and pressure sides are shown with solid and dashed black lines respectively. Locations of  $x_{LET}$  and  $x_{Flat}$  are marked by grey dotted and dash-dotted vertical lines.

**SI.5. Spanwise-averaged Navier-Stokes equations in the Flat region**

In the Flat region of the riblet samples, we use the Cartesian form of the Navier-Stokes equation in the  $x$  direction and apply the spanwise-averaging operation defined as

$$\langle \dots \rangle = \frac{1}{\lambda} \int_0^\lambda \dots dz \quad (\text{SI.5.1})$$

to get

$$\rho \left( \left\langle u \frac{\partial u}{\partial x} \right\rangle + \left\langle v \frac{\partial u}{\partial y} \right\rangle + \left\langle w \frac{\partial u}{\partial z} \right\rangle \right) = - \left\langle \frac{\partial p}{\partial x} \right\rangle + \mu \left( \left\langle \frac{\partial^2 u}{\partial x^2} \right\rangle + \left\langle \frac{\partial^2 u}{\partial y^2} \right\rangle + \left\langle \frac{\partial^2 u}{\partial z^2} \right\rangle \right) \quad (\text{SI.5.2})$$

The derivatives in the  $x$  and  $y$  direction and the averaging operation can commute thus

$$\rho \left( \left\langle u \frac{\partial u}{\partial x} \right\rangle + \left\langle v \frac{\partial u}{\partial y} \right\rangle + \left\langle w \frac{\partial u}{\partial z} \right\rangle \right) = - \frac{\partial \langle p \rangle}{\partial x} + \mu \left( \frac{\partial^2 \langle u \rangle}{\partial x^2} + \frac{\partial^2 \langle u \rangle}{\partial y^2} + \left\langle \frac{\partial^2 u}{\partial z^2} \right\rangle \right). \quad (\text{SI.5.3})$$

Using the product rule

$$\left\langle u \frac{\partial u}{\partial x} \right\rangle = \frac{\partial \langle uu \rangle}{\partial x} - \left\langle u \frac{\partial u}{\partial x} \right\rangle \quad (\text{SI.5.4})$$

$$\left\langle v \frac{\partial u}{\partial y} \right\rangle = \frac{\partial \langle uv \rangle}{\partial y} - \left\langle u \frac{\partial v}{\partial y} \right\rangle \quad (\text{SI.5.5})$$

$$\left\langle w \frac{\partial u}{\partial z} \right\rangle = \left\langle \frac{\partial (uw)}{\partial z} \right\rangle - \left\langle u \frac{\partial w}{\partial z} \right\rangle. \quad (\text{SI.5.6})$$

Due to the periodicity of the velocity in the  $z$  direction,  $u(z = \lambda) = u(z = 0)$  and  $w(z = \lambda) = w(z = 0)$  and we get

$$\left\langle \frac{\partial uw}{\partial z} \right\rangle = \frac{1}{\lambda} \int_0^\lambda \frac{\partial uw}{\partial z} dz = \frac{1}{\lambda} \left( uw \Big|_{z=0} - uw \Big|_{z=\lambda} \right) = 0 \quad (\text{SI.5.7})$$

and using equations (SI.5.4), (SI.5.5), (SI.5.6), and continuity, the left hand side of equation (SI.5.3) is simplified to

$$\rho \left( \left\langle u \frac{\partial u}{\partial x} \right\rangle + \left\langle v \frac{\partial u}{\partial y} \right\rangle + \left\langle w \frac{\partial u}{\partial z} \right\rangle \right) = \rho \left( \frac{\partial \langle uu \rangle}{\partial x} + \frac{\partial \langle uv \rangle}{\partial y} \right). \quad (\text{SI.5.8})$$

On the right hand side, with symmetry and periodicity, for  $|y| > h/2$  (see figure SI.6(a)), and the fact that outside the riblets, above the peaks, the velocity gradient needs to be continuous everywhere, we have

$$\frac{\partial u}{\partial z} \Big|_{z=\lambda^+} = \frac{\partial u}{\partial z} \Big|_{z=\lambda^-} = \frac{\partial u}{\partial z} \Big|_{z=0^+} = \frac{\partial u}{\partial z} \Big|_{z=0^-} = 0 \quad (\text{SI.5.9})$$

resulting in

$$\left\langle \frac{\partial^2 u}{\partial z^2} \right\rangle = \frac{1}{\lambda} \int_0^\lambda \frac{\partial^2 u}{\partial z^2} dz = \frac{1}{\lambda} \left( \frac{\partial u}{\partial z} \Big|_{z=\lambda} - \frac{\partial u}{\partial z} \Big|_{z=0} \right) = \frac{-2}{\lambda} \frac{\partial u}{\partial z} \Big|_{z=0} = 0 \quad (\text{SI.5.10})$$

Inside the grooves, for  $y_{\text{trough}} \leq |y| \leq h/2$ , where the walls start at a later  $z_{w1} \geq 0$  and

terminate at an earlier  $z_{w2} \leq \lambda$  (where  $\lambda - z_{w2} = z_{w1}$ , see figure SI.6(a)), with symmetry we have

$$\left\langle \frac{\partial^2 u}{\partial z^2} \right\rangle = \frac{1}{\lambda} \int_0^\lambda \frac{\partial^2 u}{\partial z^2} dz = \frac{1}{\lambda} \left( \left. \frac{\partial u}{\partial z} \right|_{z=z_{w2}^-} - \left. \frac{\partial u}{\partial z} \right|_{z=z_{w1}^+} \right) = \frac{-2}{\lambda} \left. \frac{\partial u}{\partial z} \right|_{z=z_{w1}^+} \quad (\text{SI.5.11})$$

Therefore, equation (SI.5.3) is written as

$$\rho \left( \frac{\partial \langle uu \rangle}{\partial x} + \frac{\partial \langle uv \rangle}{\partial y} \right) = -\frac{\partial \langle p \rangle}{\partial x} + \mu \left( \frac{\partial^2 \langle u \rangle}{\partial x^2} + \frac{\partial^2 \langle u \rangle}{\partial y^2} \right) + \mathcal{Z} \quad (\text{SI.5.12})$$

with

$$\mathcal{Z} = \begin{cases} -\frac{2\mu}{\lambda} \left. \frac{\partial u}{\partial z} \right|_{z=z_{w1}^+} & y_{\text{trough}} \leq |y| \leq h/2 \\ 0 & |y| > h/2. \end{cases} \quad (\text{SI.5.13})$$

Ultimately we re-write the equations in the form

$$\rho \left( \langle u \rangle \frac{\partial \langle u \rangle}{\partial x} + \langle v \rangle \frac{\partial \langle u \rangle}{\partial y} \right) = -\frac{\partial \langle P^* \rangle}{\partial x} + \mu \left( \frac{\partial^2 \langle u \rangle}{\partial y^2} \right) \quad (\text{SI.5.14})$$

where  $-\partial \langle P^* \rangle / \partial x$  is an equivalent pressure gradient term defined as

$$-\frac{\partial \langle P^* \rangle}{\partial x} = -\frac{\partial \langle p \rangle}{\partial x} + \mu \frac{\partial^2 \langle u \rangle}{\partial x^2} + \mathcal{Z} + \rho \left( \langle u \rangle \frac{\partial \langle u \rangle}{\partial x} + \langle v \rangle \frac{\partial \langle u \rangle}{\partial y} - \frac{\partial \langle uu \rangle}{\partial x} - \frac{\partial \langle uv \rangle}{\partial y} \right). \quad (\text{SI.5.15})$$

### SI.6. Spanwise-averaged Navier-Stokes equations in the curved leading edge

For a surface with the local contour curvature defined as  $\kappa(s) = 1/R(s)$  and for an incompressible fluid (Schlichting & Gersten 2016), the Navier-Stokes equation in the direction tangent to the wall is written as (see figure SI.6(b))

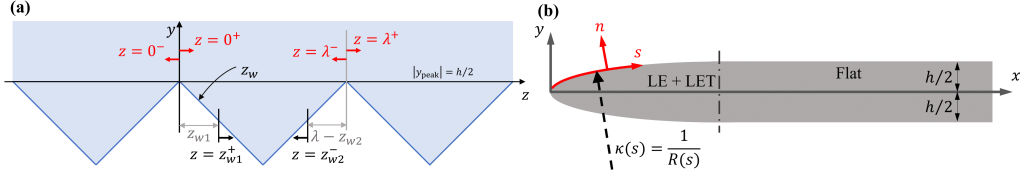


Figure SI.6: (a) Schematic of a riblet surface and the boundary conditions for characterizing the viscous diffusion in the  $z$  direction as part of the averaging operation.

(b) Schematic of the leading edge of the plate and the coordinate system tangent and normal to the wall.  $\kappa(s)$  is the local curvature of the curved leading edge and is a function of the  $s$  direction.

$$\rho \left( \frac{1}{1 + \kappa n} u_s \frac{\partial u_s}{\partial s} + v_n \frac{\partial u_s}{\partial n} + \frac{\kappa}{1 + \kappa n} u_s v_n + w \frac{\partial u_s}{\partial z} \right) = - \frac{1}{1 + \kappa n} \frac{\partial p}{\partial s} + \frac{1}{(1 + \kappa n)} \left( \frac{\partial \tau_{ss}}{\partial s} + \frac{1}{(1 + \kappa n)} \frac{\partial}{\partial n} \left[ (1 + \kappa n)^2 \tau_{sn} \right] \right) + \mu \frac{\partial^2 u_s}{\partial z^2} \quad (\text{SI.6.1})$$

where

$$\tau_{ss} = \frac{2\mu}{1 + \kappa n} \left( \frac{\partial u_s}{\partial s} + \kappa v_n \right) \quad (\text{SI.6.2})$$

and

$$\tau_{sn} = \mu \left( \frac{\partial u_s}{\partial n} - \frac{\kappa u_s}{1 + \kappa n} + \frac{1}{1 + \kappa n} \frac{\partial v_n}{\partial s} \right) \quad (\text{SI.6.3})$$

First, in the absence of riblets,  $w = 0$ ,  $\partial u_s / \partial z = 0$ , and  $\partial^2 u_s / \partial z^2 = 0$ , and the equations return back to 2D forms. Substituting equations (SI.6.2) and (SI.6.3) in the viscous diffusion terms

$$\frac{\partial \tau_{ss}}{\partial s} = \frac{2\mu}{(1 + \kappa n)} \frac{\partial^2 u_s}{\partial s^2} + \frac{2\mu\kappa}{(1 + \kappa n)} \frac{\partial v_n}{\partial s} + 2\mu\mathcal{K}' \quad (\text{SI.6.4})$$

where  $\mathcal{K}'$  combines all the terms that include the effect of the  $\partial\kappa/\partial s$ :

$$\mathcal{K}' = \frac{1}{(1 + \kappa n)^2} \left( -n \frac{\partial u_s}{\partial s} + v_n \right) \frac{\partial \kappa}{\partial s} \quad (\text{SI.6.5})$$

and

$$\left( \frac{1}{(1 + \kappa n)} \frac{\partial}{\partial n} \left[ (1 + \kappa n)^2 \tau_{sn} \right] \right) = (1 + \kappa n) \frac{\partial \tau_{sn}}{\partial n} + 2\kappa \tau_{sn} = \mu(1 + \kappa n) \frac{\partial^2 u_s}{\partial n^2} + \mu\kappa \frac{\partial u_s}{\partial n} - \frac{\kappa^2 \mu}{1 + \kappa n} u_s + \frac{\mu\kappa}{(1 + \kappa n)} \frac{\partial v_n}{\partial s} + \mu \frac{\partial^2 v_s}{\partial s \partial n} \quad (\text{SI.6.6})$$

Adding the two viscous terms of equations (SI.6.4) and (SI.6.6) together and collecting and reorganizing some of the terms and dividing by  $(1 + \kappa n)$

$$\begin{aligned} & \mu \left( \frac{\partial^2 u_s}{\partial s^2} + \frac{\partial^2 u_s}{\partial n^2} \right) + \frac{\mu}{(1 + \kappa n)} \frac{\partial}{\partial s} \left( \frac{1}{1 + \kappa n} \frac{\partial u_s}{\partial s} + \frac{\partial v_n}{\partial n} + \frac{\kappa}{1 + \kappa n} v_n \right) + \frac{\mu \mathcal{K}'}{(1 + \kappa n)} + \\ & \mu \left( \frac{(-2\kappa n - \kappa^2 n^2)}{(1 + \kappa n)^2} \frac{\partial^2 u_s}{\partial s^2} + \frac{\kappa}{(1 + \kappa n)} \frac{\partial u_s}{\partial n} + \frac{2\kappa}{(1 + \kappa n)^2} \frac{\partial v_n}{\partial s} - \frac{\kappa^2}{(1 + \kappa n)^2} u_s \right) \end{aligned} \quad (\text{SI.6.7})$$

where continuity dictates that

$$\left( \frac{1}{1 + \kappa n} \frac{\partial u_s}{\partial s} + \frac{\partial v_n}{\partial n} + \frac{\kappa}{1 + \kappa n} v_n \right) = -\frac{\partial w}{\partial z} \quad (\text{SI.6.8})$$

and for 2D flows,  $\partial w / \partial z = 0$ . As for the pressure gradient term:

$$-\frac{1}{1 + \kappa n} \frac{\partial p}{\partial s} = -\frac{\partial p}{\partial s} + \frac{\kappa n}{1 + \kappa n} \frac{\partial p}{\partial s} \quad (\text{SI.6.9})$$

and thus the right hand side is simplified to

$$\begin{aligned} & -\frac{\partial p}{\partial s} + \mu \left( \frac{\partial^2 u_s}{\partial s^2} + \frac{\partial^2 u_s}{\partial n^2} \right) + \frac{\kappa n}{1 + \kappa n} \frac{\partial p}{\partial s} + \frac{\mu \mathcal{K}'}{(1 + \kappa n)} + \\ & \mu \left( \frac{(-2\kappa n - \kappa^2 n^2)}{(1 + \kappa n)^2} \frac{\partial^2 u_s}{\partial s^2} + \frac{\kappa}{(1 + \kappa n)} \frac{\partial u_s}{\partial n} + \frac{2\kappa}{(1 + \kappa n)^2} \frac{\partial v_n}{\partial s} - \frac{\kappa^2}{(1 + \kappa n)^2} u_s \right). \end{aligned} \quad (\text{SI.6.10})$$

As for the left hand side, we can rewrite the terms in the form:

$$\begin{aligned} & \rho \left( \frac{1}{1 + \kappa n} u_s \frac{\partial u_s}{\partial s} + v_n \frac{\partial u_s}{\partial n} + \frac{\kappa}{1 + \kappa n} u_s v_n \right) = \\ & \rho \left( u_s \frac{\partial u_s}{\partial s} + v_n \frac{\partial u_s}{\partial n} \right) - \rho \left( \frac{\kappa n}{1 + \kappa n} u_s \frac{\partial u_s}{\partial s} - \frac{\kappa}{1 + \kappa n} u_s v_n \right) \end{aligned} \quad (\text{SI.6.11})$$

Thus equation (SI.6.1) is re-arranged as

$$\rho \left( u_s \frac{\partial u_s}{\partial s} + v_n \frac{\partial u_s}{\partial n} \right) = -\frac{\partial p}{\partial s} + \mu \left( \frac{\partial^2 u_s}{\partial s^2} + \frac{\partial^2 u_s}{\partial n^2} \right) + \mathcal{K}_1 \quad (\text{SI.6.12})$$

where  $\mathcal{K}_1$  captures all the terms involving the curvature term  $\kappa$ :

$$\begin{aligned} \mathcal{K}_1 = & \rho \left( \frac{\kappa n}{1 + \kappa n} u_s \frac{\partial u_s}{\partial s} - \frac{\kappa}{1 + \kappa n} u_s v_n \right) + \frac{\kappa n}{1 + \kappa n} \frac{\partial p}{\partial s} + \frac{\mu \mathcal{K}'}{(1 + \kappa n)} + \\ & \mu \left( \frac{(-2\kappa n - \kappa^2 n^2)}{(1 + \kappa n)^2} \frac{\partial^2 u_s}{\partial s^2} + \frac{\kappa}{(1 + \kappa n)} \frac{\partial u_s}{\partial n} + \frac{2\kappa}{(1 + \kappa n)^2} \frac{\partial v_n}{\partial s} - \frac{\kappa^2}{(1 + \kappa n)^2} u_s \right). \end{aligned} \quad (\text{SI.6.13})$$

Similar to appendix SI.5 we can rewrite equation (SI.6.12) in the form of

$$\rho \left( u_s \frac{\partial u_s}{\partial s} + v_n \frac{\partial u_s}{\partial n} \right) = -\frac{\partial P^*}{\partial s} + \mu \left( \frac{\partial^2 u_s}{\partial n^2} \right) \quad (\text{SI.6.14})$$

where the equivalent pressure gradient term is

$$-\frac{\partial P^*}{\partial s} = -\frac{\partial p}{\partial s} + \mu \left( \frac{\partial^2 u_s}{\partial s^2} \right) + \mathcal{K}_1 \quad (\text{SI.6.15})$$

and in the absence of curvature,  $\kappa \rightarrow 0$  and  $\partial\kappa/\partial s \rightarrow 0$ ,  $\mathcal{K}_1$  becomes zero and the equations return back to that of the BL over the flat surface. Hence, in the curved region of the elliptical leading edge, prior to the appearance of the riblets, the  $-\partial P^*/\partial s$  term includes contributions from the pressure gradient, the viscous diffusion terms in the streamwise direction, as well as the curvature related terms as shown above and thus the  $m$  parameter of the FS fit for the velocity profiles will capture the effect of these components.

Now for the textured portion of the curved leading edge, or LET, we apply the spanwise-averaging operation to the right hand side of equation (SI.6.1), and cannot neglect the effect of the out of plane components:

$$\left\langle \rho \left( \frac{1}{1+\kappa n} u_s \frac{\partial u_s}{\partial s} + v_n \frac{\partial u_s}{\partial n} + \frac{\kappa}{1+\kappa n} u_s v_n + w \frac{\partial u_s}{\partial z} \right) \right\rangle = \quad (\text{SI.6.16})$$

$$\rho \left( \frac{1}{1+\kappa n} \left\langle u_s \frac{\partial u_s}{\partial s} \right\rangle + \left\langle v_n \frac{\partial u_s}{\partial n} \right\rangle + \left\langle w \frac{\partial u_s}{\partial z} \right\rangle + \frac{\kappa}{1+\kappa n} \langle u_s v_n \rangle \right)$$

where using the product rule we substitute the first two terms with

$$\left\langle u_s \frac{\partial u_s}{\partial s} \right\rangle = \frac{\partial \langle u_s u_s \rangle}{\partial s} - \left\langle u_s \frac{\partial u_s}{\partial s} \right\rangle, \quad (\text{SI.6.17})$$

$$\left\langle v_n \frac{\partial u_s}{\partial n} \right\rangle = \frac{\partial \langle u_s v_n \rangle}{\partial s} - \left\langle u_s \frac{\partial v_n}{\partial n} \right\rangle \quad (\text{SI.6.18})$$

$$\left\langle w \frac{\partial u_s}{\partial z} \right\rangle = \left\langle \frac{\partial u_s w}{\partial s} \right\rangle - \left\langle u_s \frac{\partial w}{\partial z} \right\rangle \quad (\text{SI.6.19})$$

where using similar integral operation as discussed in appendix SI.5 in equation (SI.5.7),

$$\left\langle \frac{\partial u_s w}{\partial s} \right\rangle = 0 \quad (\text{SI.6.20})$$

Then, multiplying the continuity equation with  $u_s$  and applying the spanwise-averaging operation we can write:

$$\frac{1}{1+\kappa n} \left\langle u_s \frac{\partial u_s}{\partial s} \right\rangle + \left\langle u_s \frac{\partial v_n}{\partial n} \right\rangle + \left\langle u_s \frac{\partial w}{\partial z} \right\rangle = -\frac{\kappa}{1+\kappa n} \langle u_s v_n \rangle \quad (\text{SI.6.21})$$

and thus using equations (SI.6.17), (SI.6.18), and (SI.6.21), we rewrite (SI.6.16) as

$$\rho \left( \frac{1}{1+\kappa n} \frac{\partial \langle u_s u_s \rangle}{\partial s} + \frac{\partial \langle u_s v_n \rangle}{\partial n} + \frac{2\kappa}{1+\kappa n} \langle u_s v_n \rangle \right) \quad (\text{SI.6.22})$$

which similar to earlier it can be divided into:

$$\rho \left( \frac{\partial \langle u_s u_s \rangle}{\partial s} + \frac{\partial \langle u_s v_n \rangle}{\partial n} \right) + \rho \left( -\frac{\kappa n}{1+\kappa n} \frac{\partial \langle u_s u_s \rangle}{\partial s} + \frac{2\kappa}{1+\kappa n} \langle u_s v_n \rangle \right) \quad (\text{SI.6.23})$$

As for the left hand side, following similar steps as before, using equations (SI.6.7) and (SI.6.8), we can write the viscous terms as

$$\begin{aligned}
& \left\langle \frac{1}{(1+\kappa n)} \left( \frac{\partial \tau_{ss}}{\partial s} + \frac{1}{(1+\kappa n)} \frac{\partial}{\partial n} [(1+\kappa n)^2 \tau_{sn}] \right) + \mu \frac{\partial^2 u_s}{\partial z^2} \right\rangle = \\
& \mu \left( \frac{\partial^2 \langle u_s \rangle}{\partial s^2} + \frac{\partial^2 \langle u_s \rangle}{\partial n^2} + \left\langle \frac{\partial^2 u_s}{\partial z^2} \right\rangle \right) - \frac{\mu}{1+\kappa n} \frac{\partial}{\partial s} \left\langle \frac{\partial w}{\partial z} \right\rangle + \frac{\mu \langle \mathcal{K}' \rangle}{(1+\kappa n)} + \\
& \mu \left( \frac{(-2\kappa n - \kappa^2 n^2)}{(1+\kappa n)^2} \frac{\partial^2 \langle u_s \rangle}{\partial s^2} + \frac{\kappa}{(1+\kappa n)} \frac{\partial \langle u_s \rangle}{\partial n} + \frac{2\kappa}{(1+\kappa n)^2} \frac{\partial \langle v_n \rangle}{\partial s} - \frac{\kappa^2}{(1+\kappa n)^2} \langle u_s \rangle \right)
\end{aligned} \tag{SI.6.24}$$

where

$$\left\langle \frac{\partial w}{\partial z} \right\rangle = \frac{1}{\lambda} \int_0^\lambda \frac{\partial w}{\partial z} dz = w(\lambda) - w(0) = 0 \tag{SI.6.25}$$

and similar to (SI.5.13) in appendix SI.5

$$\mu \left\langle \frac{\partial^2 u_s}{\partial z^2} \right\rangle = \mathcal{Z} = \begin{cases} -\frac{2\mu}{\lambda} \frac{\partial u_s}{\partial z} \Big|_{z=z_w^+} & n_{\text{trough}} \leq n \leq n_{\text{peak}} \\ 0 & |n| > n_{\text{peak}}. \end{cases} \tag{SI.6.26}$$

As for the pressure gradient term similarly:

$$-\frac{1}{1+\kappa n} \frac{\partial \langle p \rangle}{\partial s} = -\frac{\partial \langle p \rangle}{\partial s} + \frac{\kappa n}{1+\kappa n} \frac{\partial \langle p \rangle}{\partial s} \tag{SI.6.27}$$

and thus

$$\rho \left( \langle u_s \rangle \frac{\partial \langle u_s \rangle}{\partial s} + \langle v_n \rangle \frac{\partial \langle u_s \rangle}{\partial n} \right) = -\frac{\partial \langle P^* \rangle}{\partial s} + \mu \left( \frac{\partial^2 \langle u_s \rangle}{\partial n^2} \right) \tag{SI.6.28}$$

where

$$\begin{aligned}
-\frac{\langle P^* \rangle}{\partial s} &= -\frac{\partial \langle p \rangle}{\partial s} + \mu \left( \frac{\partial^2 \langle u_s \rangle}{\partial s^2} \right) + \mathcal{Z} + \mathcal{K}_2 + \\
\rho \left( \langle u_s \rangle \frac{\partial \langle u_s \rangle}{\partial s} + \langle v_n \rangle \frac{\partial \langle u_s \rangle}{\partial n} - \frac{\partial \langle u_s u_s \rangle}{\partial s} - \frac{\partial \langle u_s v_n \rangle}{\partial n} \right)
\end{aligned} \tag{SI.6.29}$$

and

$$\begin{aligned}
\mathcal{K}_2 &= \rho \left( \frac{\kappa n}{1+\kappa n} \frac{\partial \langle u_s u_s \rangle}{\partial s} - \frac{2\kappa}{1+\kappa n} \langle u_s v_n \rangle \right) + \frac{\kappa n}{1+\kappa n} \frac{\partial \langle p \rangle}{\partial s} + \frac{\mu \langle \mathcal{K}' \rangle}{(1+\kappa n)} + \\
& \mu \left( \frac{(-2\kappa n - \kappa^2 n^2)}{(1+\kappa n)^2} \frac{\partial^2 \langle u_s \rangle}{\partial s^2} + \frac{\kappa}{(1+\kappa n)} \frac{\partial \langle u_s \rangle}{\partial n} + \frac{2\kappa}{(1+\kappa n)^2} \frac{\partial \langle v_n \rangle}{\partial s} - \frac{\kappa^2}{(1+\kappa n)^2} \langle u_s \rangle \right) = \\
& \langle \mathcal{K}_1 \rangle - \frac{\rho \kappa}{1+\kappa n} \langle u_s v_n \rangle.
\end{aligned} \tag{SI.6.30}$$

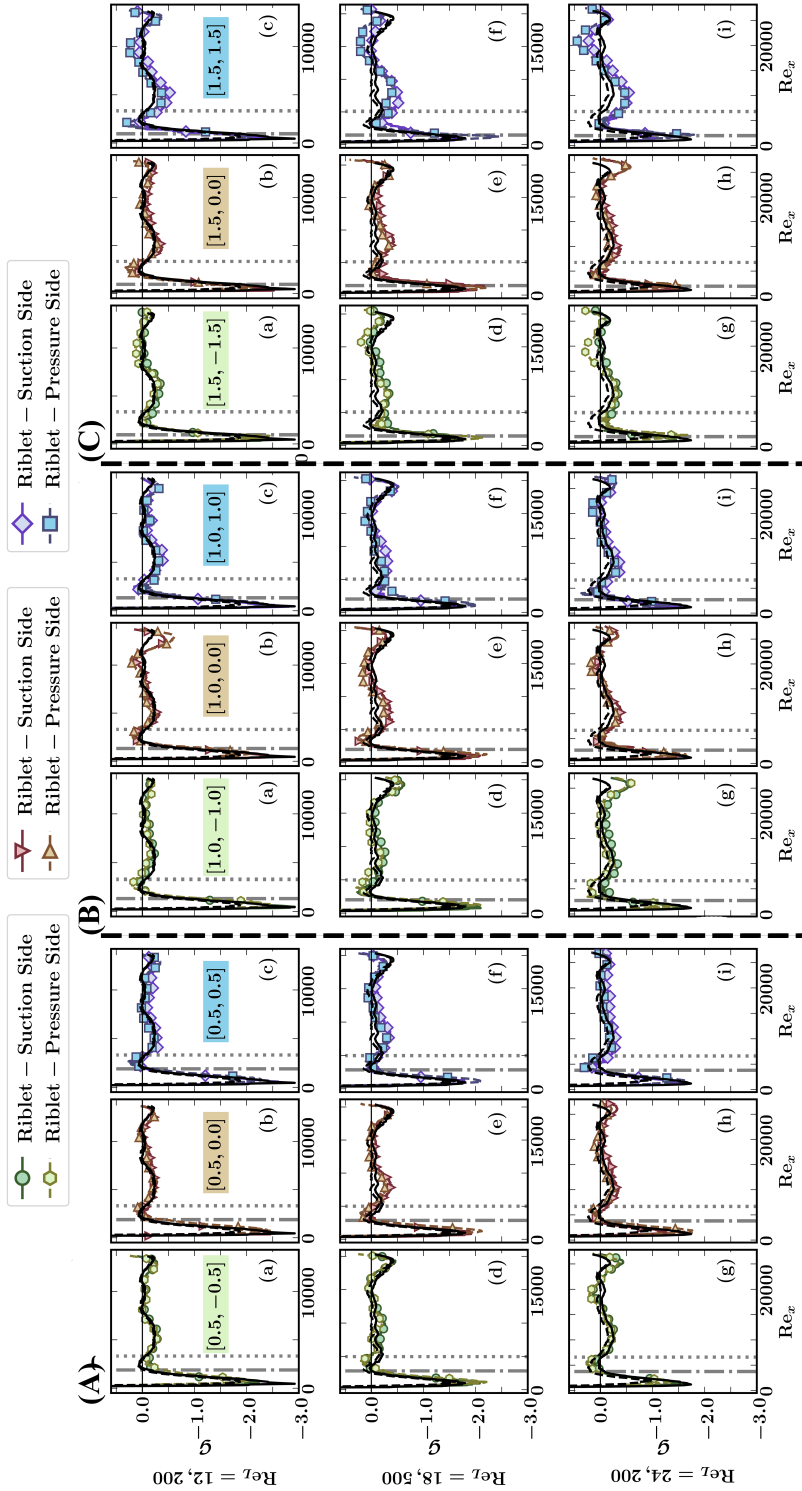
SI.7. Distribution of  $\mathcal{G}$  for all the samples

Figure SI.7: Distribution of  $\mathcal{G}$  or difference between the  $\partial(P^*/\partial x)$  and  $\partial(p)/\partial x$  terms in dimensionless form, for all the riblet samples of (A)  $\mathcal{R} = 0.5$ , (B)  $\mathcal{R} = 1.0$ , and (C)  $\mathcal{R} = 1.5$  on the suction and pressure sides of the riblet samples. The results for the smooth reference for all the tested Reynolds numbers are shown with solid and dashed black lines for the suction and pressure sides respectively. Locations of  $x_{\text{LET}}$  and  $x_{\text{Flat}}$  are marked by grey dotted and dash-dotted vertical lines.

SI.8. Distribution of the effective origin for all the samples

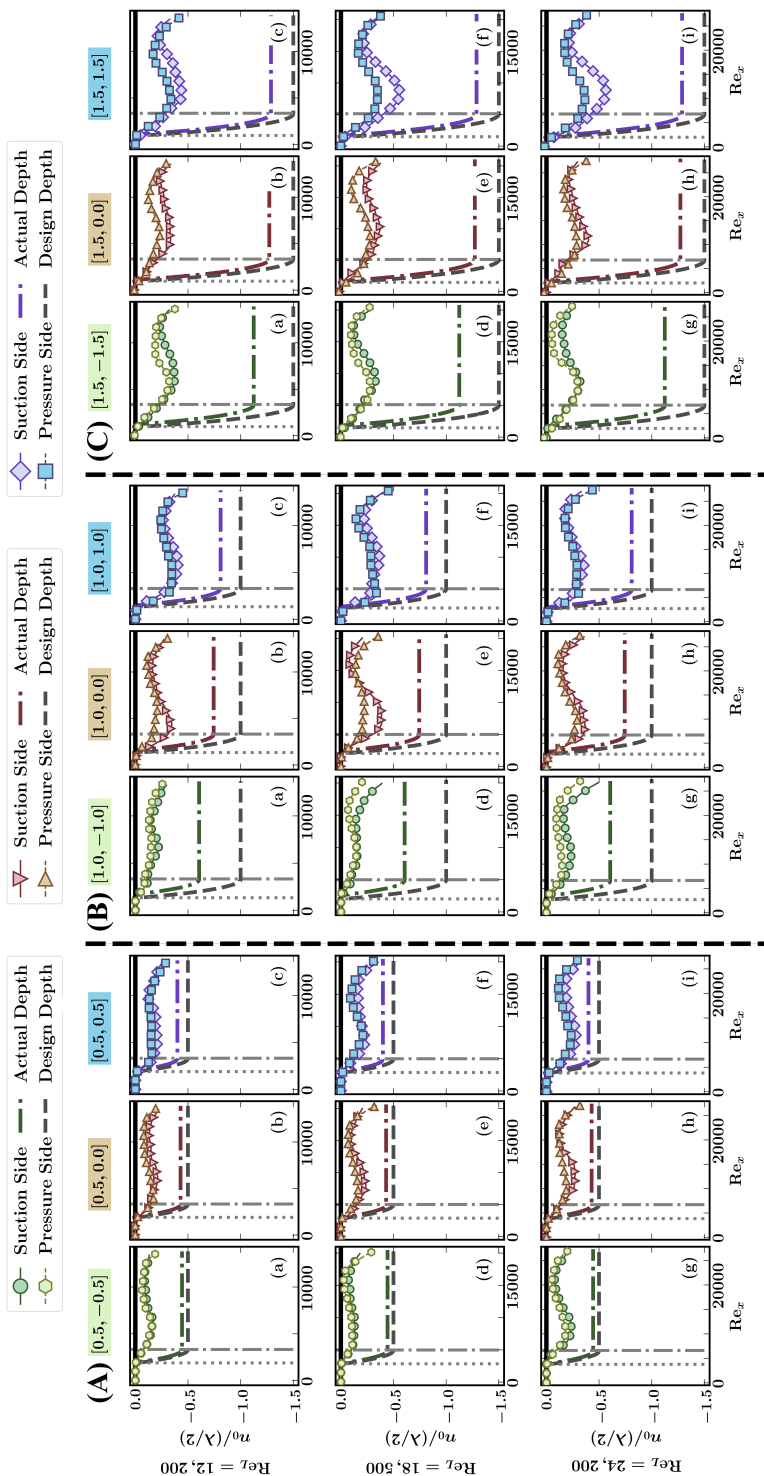


Figure SI.8: Distribution of the effective origin,  $n_0$ , for all the riblet samples of (A)  $\mathcal{R} = 0.5$ , (B)  $\mathcal{R} = 1.0$ , and (C)  $\mathcal{R} = 1.5$  on the suction and pressure sides for all the tested Reynolds numbers. Location of the design and measured troughs are also marked on the figures. Locations of  $x_{LET}$  and  $x_{Flat}$  are marked by grey dotted and dash-dotted vertical lines.

SI.9. Distribution of the boundary layer thickness,  $\delta_{99}$ , for all the samples

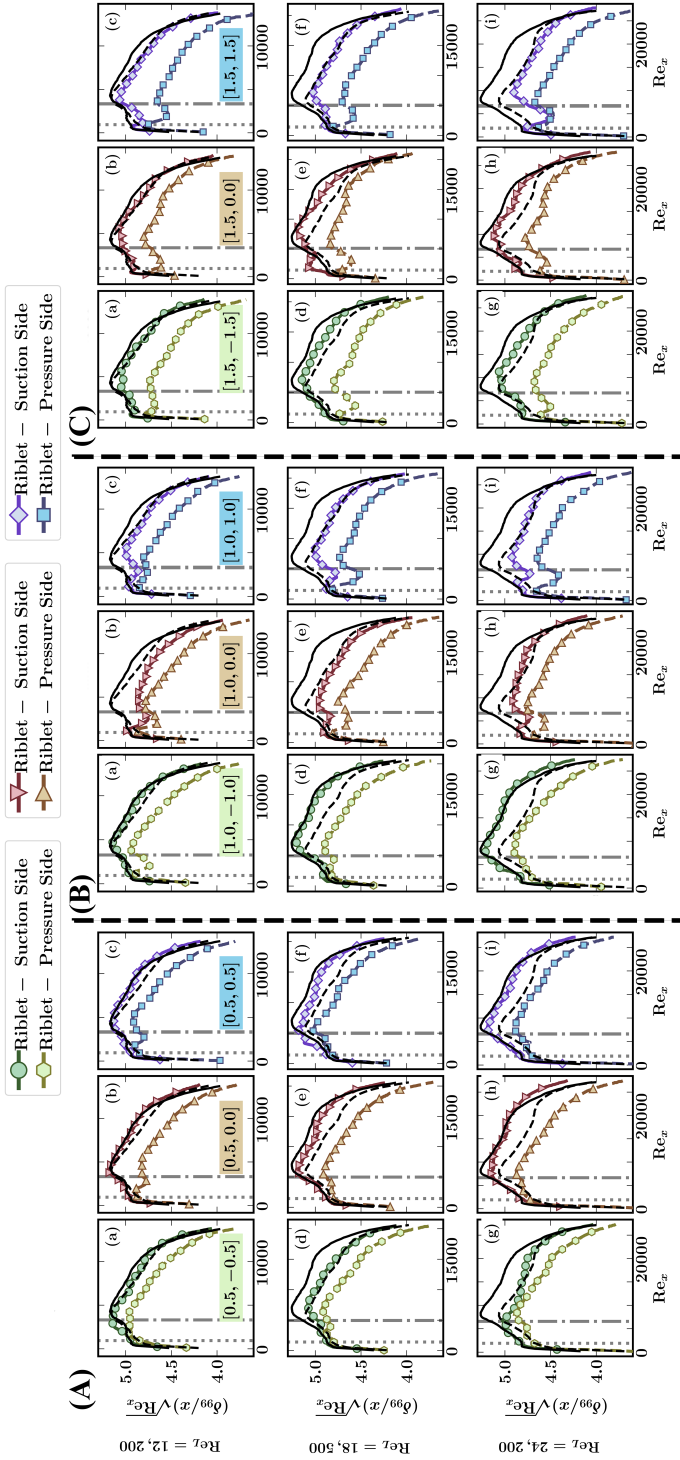


Figure SI.9: Distribution of the BL thickness,  $\delta_{99}$ , normalized by local  $x/\sqrt{Re_x}$ , for all the riblet samples of (A)  $\mathcal{R} = 0.5$ , (B)  $\mathcal{R} = 1.0$ , and (C)  $\mathcal{R} = 1.5$  on the suction and pressure sides for all the tested Reynolds numbers. The  $\delta_{99}$  of the smooth reference on the suction and pressure sides are shown with solid and dashed black lines respectively. Locations of  $x_{LET}$  and  $x_{FLAT}$  are marked by grey dotted and dash-dotted vertical lines.

REFERENCES

SCHLICHTING, HERMANN & GERSTEN, KLAUS 2016 *Boundary-layer theory*. springer.